THE USE OF SATELLITE DATA IN DIAGNOSING NWP MODEL PARAMETRIZATION PROBLEMS

E. Klinker and J.-J. Morcrette (ECMWF)

1. INTRODUCTION

For a numerical weather prediction model, such as the one operationally run for 10 day forecasts at ECMWF, the routine verification of parameters in the free atmosphere in terms of anomaly correlation or in terms of r.m.s. errors is certainly an important tool for assessing the performance of the forecasting system. In addition to the objective scores, the verification of the so-called meteorological products (2m temperature, 10 m wind, total cloudiness, precipitation) against synoptic observations of the same quantities provide somewhat more specific insight into the quality of the parametrizations of subgrid physical processes. However, a more precise evaluation of such parametrizations usually requires consideration from different perspectives. For example, apart from judging how modifications of the radiation parametrization influence large scale flow features by the model, the radiation transfer scheme can be checked by comparing its outputs for well defined atmospheric profiles with radiative fluxes and heating rate profiles computed by state-of-the-art line-by-line or narrow-band models, taken as a reference, at least in a relative sense. This approach has been adopted for the Intercomparison of Radiation Codes in Climate Models (ICRCCM; Morcrette , 1991a), The physical parametrizations can also be validated by trying to reproduce with the model a set of well documented observations that have been produced by specially designed observation experiments (as it was recently done for FIFE (Betts et al., 1993) or as it will or might be done for ICE/EUCREX, ASTEX, TOGA/COARE, ...). The comparison of model outputs with satellite observations, with their potentially good temporal and spatial coverage, offers another avenue for the validation/verification of the model physics. This paper summarizes some efforts recently made at using satellite observations for validating different aspects of the representation of the cloud-radiation interactions in the ECMWF model.

2. VALIDATION OF RADIATION

2.1 Greenhouse function

A general estimate of the quality of the model generated radiation fluxes can be obtained by comparing their statistical properties as a function of suitable boundary conditions. One commonly used parameter is the greenhouse effect of the atmosphere, which describes the amount of long wave radiation trapped in the atmosphere. By defining the greenhouse function

$$G=\frac{I}{OLR} \qquad (1)$$

as the ratio between the radiation emitted from the surface ($I=\sigma T_s^4$) and the outgoing long-wave radiation at the top of the atmosphere (OLR), the effect of the sea surface temperature is largely reduced. In this formulation the greenhouse function depends mainly on cloud cover, precipitable water and on the vertical temperature gradient in the atmosphere.

The influence of clouds can be excluded by considering only clear sky radiation fluxes. Though the procedure to derive clear sky fluxes from satellite measurements differs from model calculations, the agreement between the two is generally fairly good. The greenhouse function for clear sky fluxes at the top of the atmosphere is shown as a scatter diagram over the sea surface temperature (SST). Both the model values (Fig. 1 a) and the values calculated from ERBE measurements (Fig. 1b) show a general increase with temperature due to the water vapour feedback. In the tropical convergence zone horizontal moisture fluxes contribute to an additional increase of precipitable water, which explains the nonlinear increase of the greenhouse function at high temperatures. In these temperature ranges of the sea surface the greenhouse function calculated from model values and observed values agrees quite well.

At lower temperature ranges the model greenhouse function differs noticeably from observation. The separation of the distribution into two branches exhibits the dependence of the greenhouse function on the vertical temperature gradient in the extra-tropics (Webb et al., 1993). Similar to Slingo et al. (paper in this volume) the Southern Hemisphere values have been plotted with different symbols compared to Northern Hemisphere values. The points with a larger vertical temperature gradient in the winter hemisphere have a larger greenhouse function than points for the same SST with a smaller vertical temperature gradient in the summer hemisphere. Whereas the summer hemisphere model

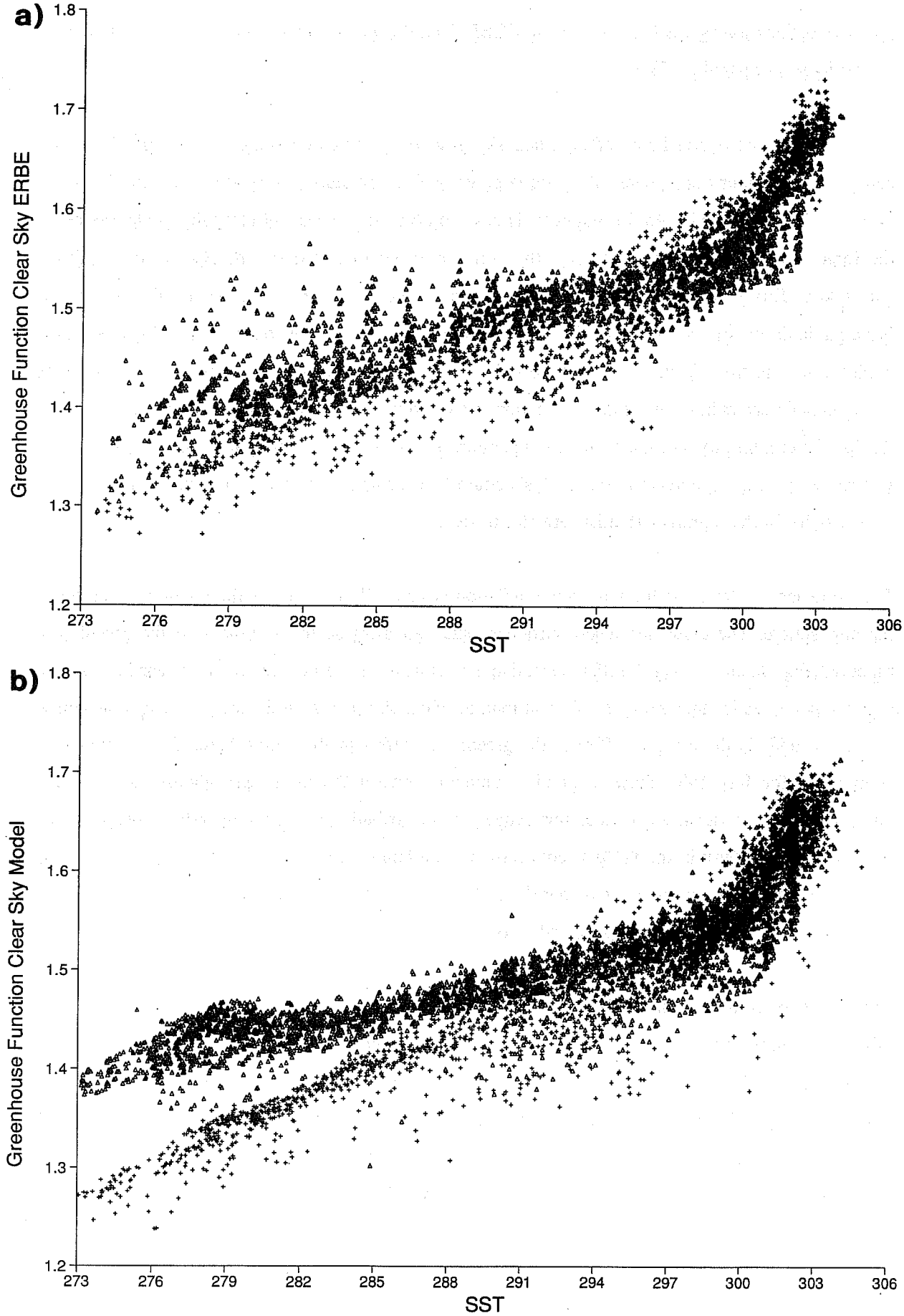

Fig. 1: Scatter diagram of the greenhouse function versus the sea surface temperature for clear sky conditions. (a) using OLR from ERBE of July 1987, (b) using OLR from short range model forecasts based on the re-analysis of July 1987. Southern Hemisphere values triangles, Northern Hemisphere values crosses.

greenhouse function agrees fairly closely to ERBE data, the winter hemisphere model values seem to be too large compared to ERBE.

The reason for an overestimate of the clear sky greenhouse function suggests two possible error sources in the winter hemisphere, either too large vertical temperature gradients or excessive humidity or a combination of both. As the diagnosis is based on 6 hour forecasts of clear sky model radiation, the forecast range is short enough that the radiation calculation reflects the state of the analyzed atmosphere. However, the southern hemispheric oceans are data sparse areas where the 6-hour forecast has a particularly large influence on the vertical gradient of the analyzed temperature. The systematic model errors in the mid-latitudes of the Southern Hemisphere are in fact in the direction that they would explain errors in the greenhouse function arising from two problems. In the short range forecast the low level humidity and the vertical temperature gradient in the troposphere increase. Excessive vertical temperature gradients in the analysis could then contribute to the systematic model error of over-activity in the Southern Hemisphere storm track.

The influence of clouds on the long-wave radiation is generally to enhance the greenhouse effect of the atmosphere. The cloud influence introduces such an increase in the scatter of the greenhouse function (Fig. 2a and b) that the SST dependence is almost lost. However, the nonlinear increase at high temperatures is much more significant than for clear sky fluxes. In the areas of deep convection the clouds add in the order of 50% to the greenhouse effect of the atmosphere. The simultaneous comparison for July 1987 shows a good agreement between the model greenhouse function and observation over most surface temperature ranges. The distribution at high temperatures suggests that the convective activity in the ITCZ is concentrated in a temperature band which is too narrow. This can also be interpreted in such a way that the model has a rather sharp threshold for deep convection at around 300 K that does not correspond to observation.

The model development can be further judged from the distribution of the greenhouse function for subsequent summer months (Fig. 3). In general the agreement between different years and ERBE values from 1987 is reasonably good. The largest differences are found at high SST's. As the re-analysis of July 1987 was carried out with a model formulation of mid-1991, it is not surprising that the greenhouse function for July 1991 is very similar to the greenhouse function for July 1987. During 1992 and 1993, when the high resolution model T213 has been in operational use a further narrowing of the SST range, where deep convection occurs, suggests an increasing problem in the spatial distribution of convection.

Whereas the greenhouse effect in July 1991 has been overestimated the July 1993 values represent a

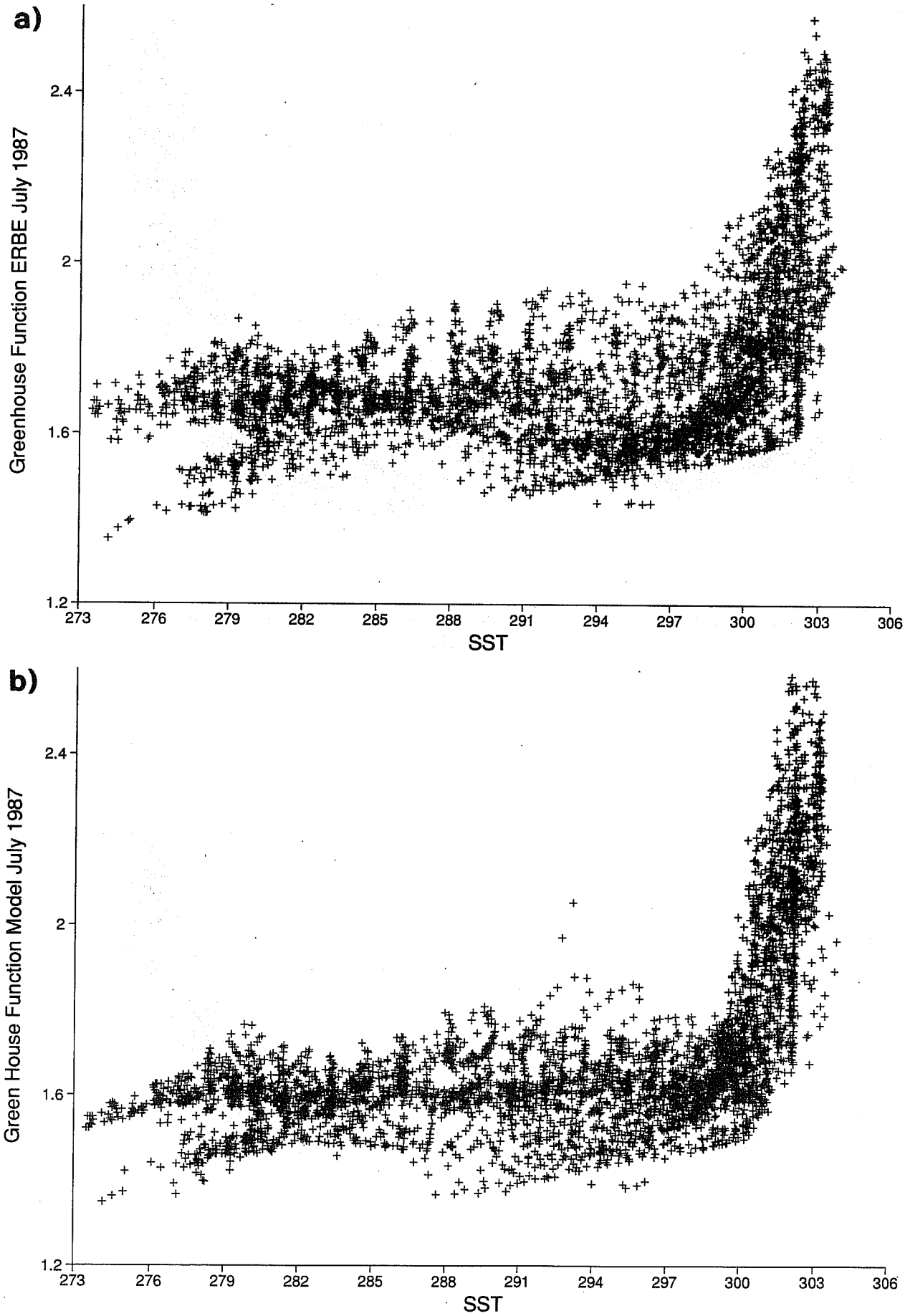

Fig. 2: Scatter diagram of the greenhouse function versus the sea surface temperature. (a) using OLR from ERBE of July 1987, (b) using OLR from short range model forecasts based on the re-analysis of July 1987.

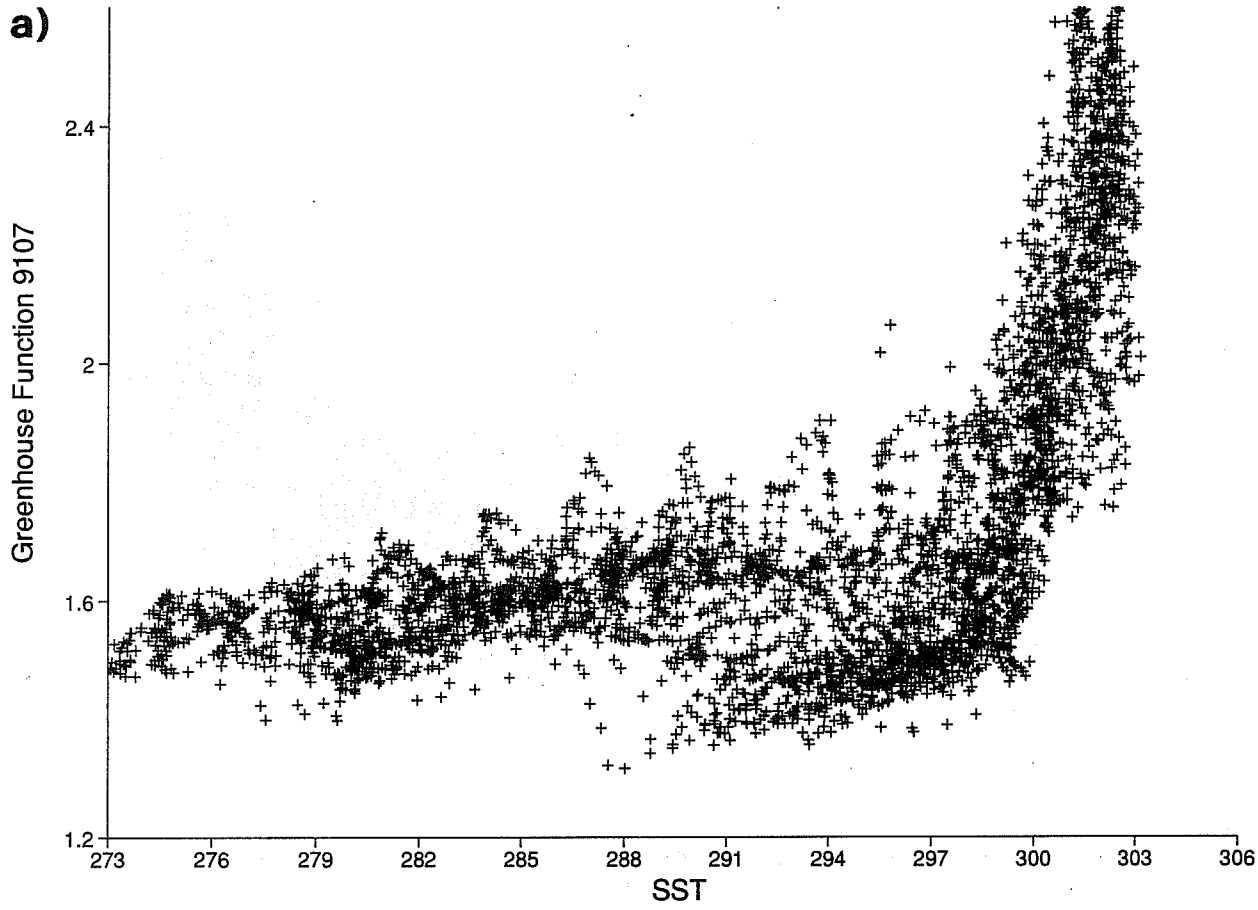

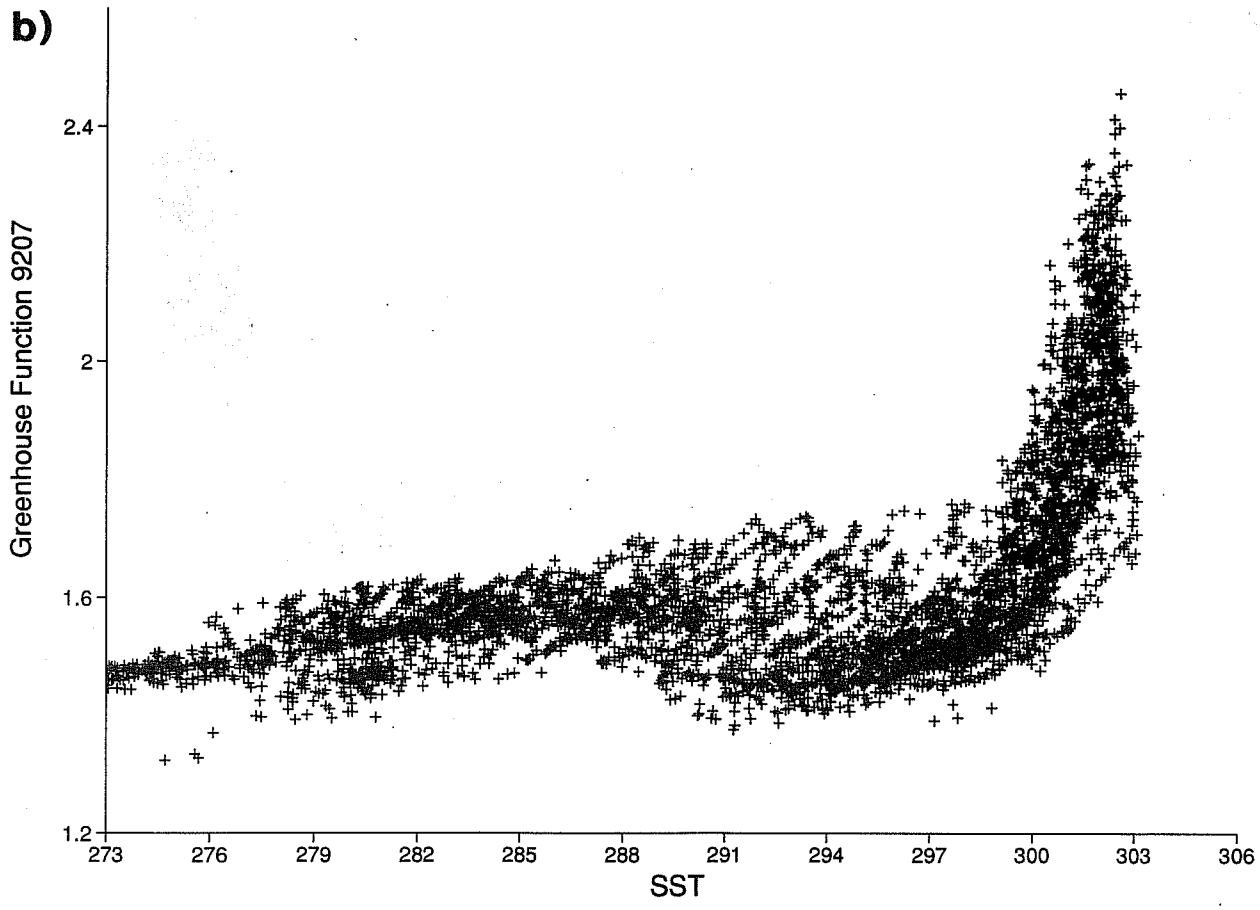

Fig. 3: Scatter diagram of the greenhouse function versus the sea surface temperature using OLR from operational ECMWF short range forecasts. (a) July 1991, (b) July 1992, (c) July 1993.

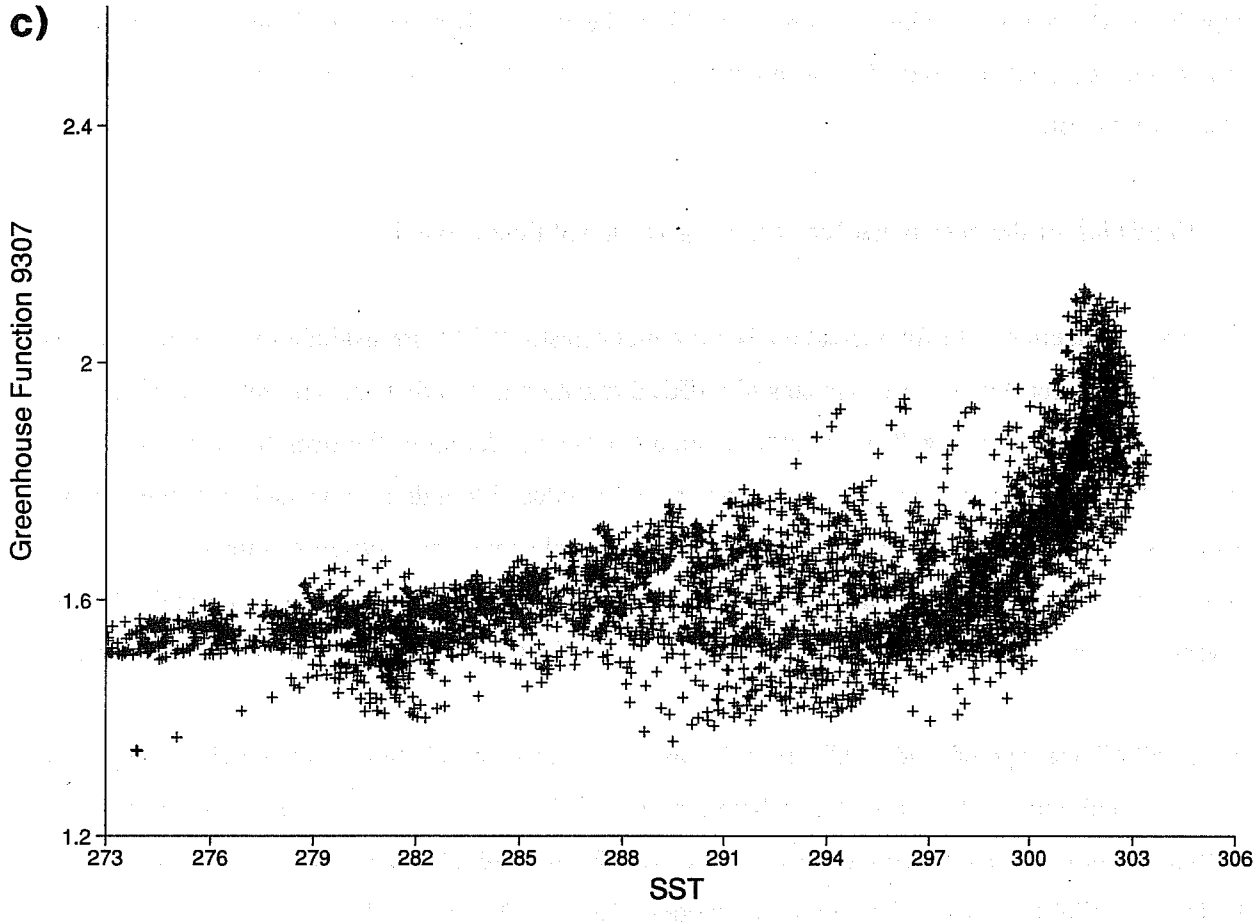
c)
Greenhouse Function 9307
2.4
2
1.6
1.2
273
276
279
282
285
288
291
294
297
300
303
306
SST

large underestimation. Too high values of OLR have been a problem since the definition of the liquid water content of cirrus clouds has been changed from a fixed number to a fraction of the saturation mass mixing ratio.

2.1 Validation of the operational forecast using zonal and time mean data

The use of satellite data for validation is very much restricted by its availability in time. This is especially true for high quality data sets like ERBE radiation fluxes that are only released after time consuming post-processing. This excludes a simultaneous validation of the operational model. For a non-simultaneous application the information has to be reduced to a dimension such that inter-annual variations are less important. Even on a monthly mean scale convective systems in the tropics, which produce strong cloud-radiation interaction, show regional inter-annual variations which require further averaging in space if the radiative fluxes can only be validated against a limited reference data set.

At ECMWF one type of model validation is based on averaging radiation fluxes longitudinally over sea and land points. The differences between model fluxes and observations are calculated by subtracting monthly and longitudinal averages of ERBE fluxes of a fixed annual cycle (February 1985 to January 1986) from the time series of model fluxes. Differences between model and ERBE outgoing long-wave radiation at the top of the atmosphere over sea points are shown in Fig. 4.

A marked change in the performance of the model occurred in May 1989 when a new radiation scheme (Morcrette, 1990) and the new mass flux scheme for convection (Tiedtke, 1989) were introduced at ECMWF. The more realistic radiative response to clouds together with an improved description of the deep convection in the tropics resulted in a better representation of the OLR minimum along the tropical convergence zone.

A model change in June 1990 had a significant impact on cloud cover. The increase of sea surface fluxes in low wind speed situations increased the moisture available for cloud formation. A more direct effect on cloud cover was achieved by including not only precipitating but also shallow non-precipitating cumuli in the input for the radiation calculation. Without changing the optical properties of clouds those model modifications lead to an underestimation of the OLR in the tropics. The differences between model values and ERBE measurements increased further after the assumption of how multilevel clouds should overlap had been changed in April 1991.

The change to a high resolution model T213 in the horizontal and to 31 levels in the vertical brought an improvement in the representation of tropical OLR in the forecast, though the negative bias in the

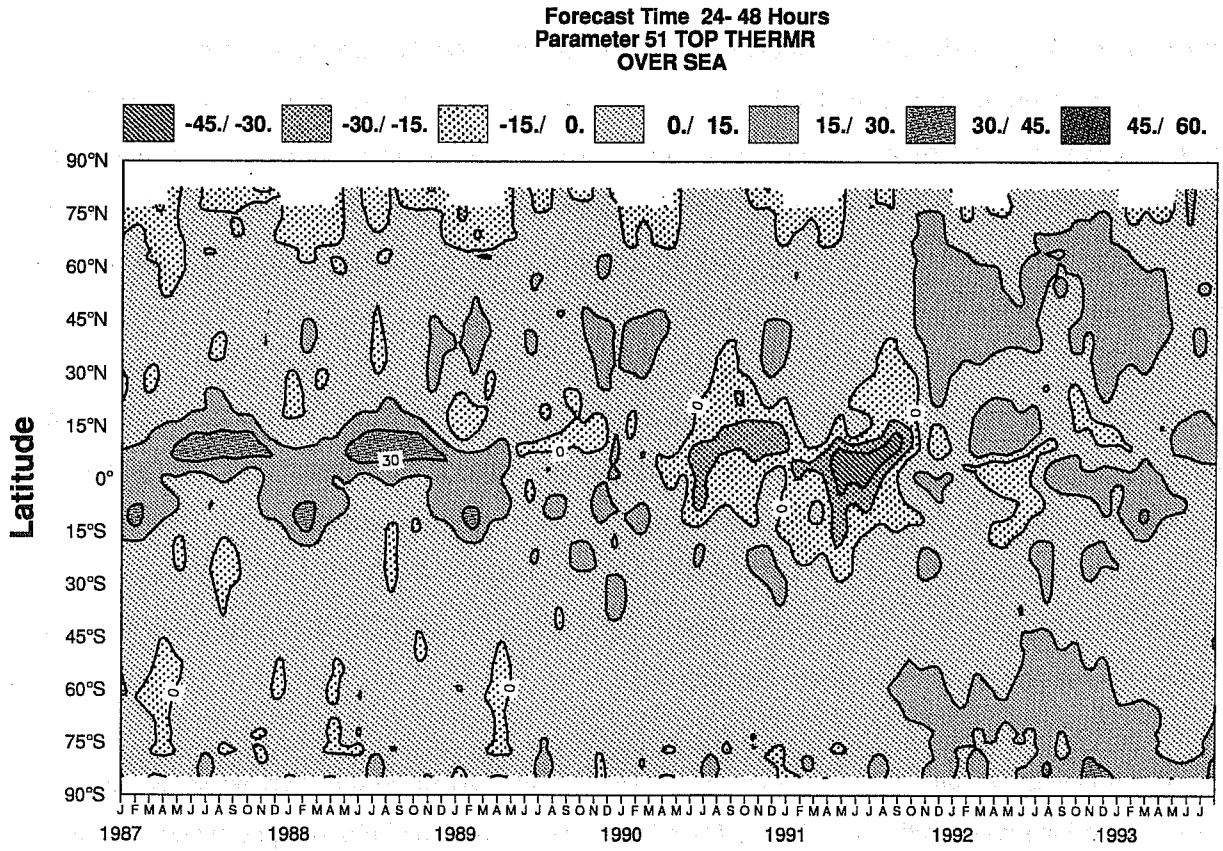

Fig. 4: Monthly and zonal mean differences between ERBE and model OLR. Zonal averages are calculated for sea points only. Units: Watts/m^2.

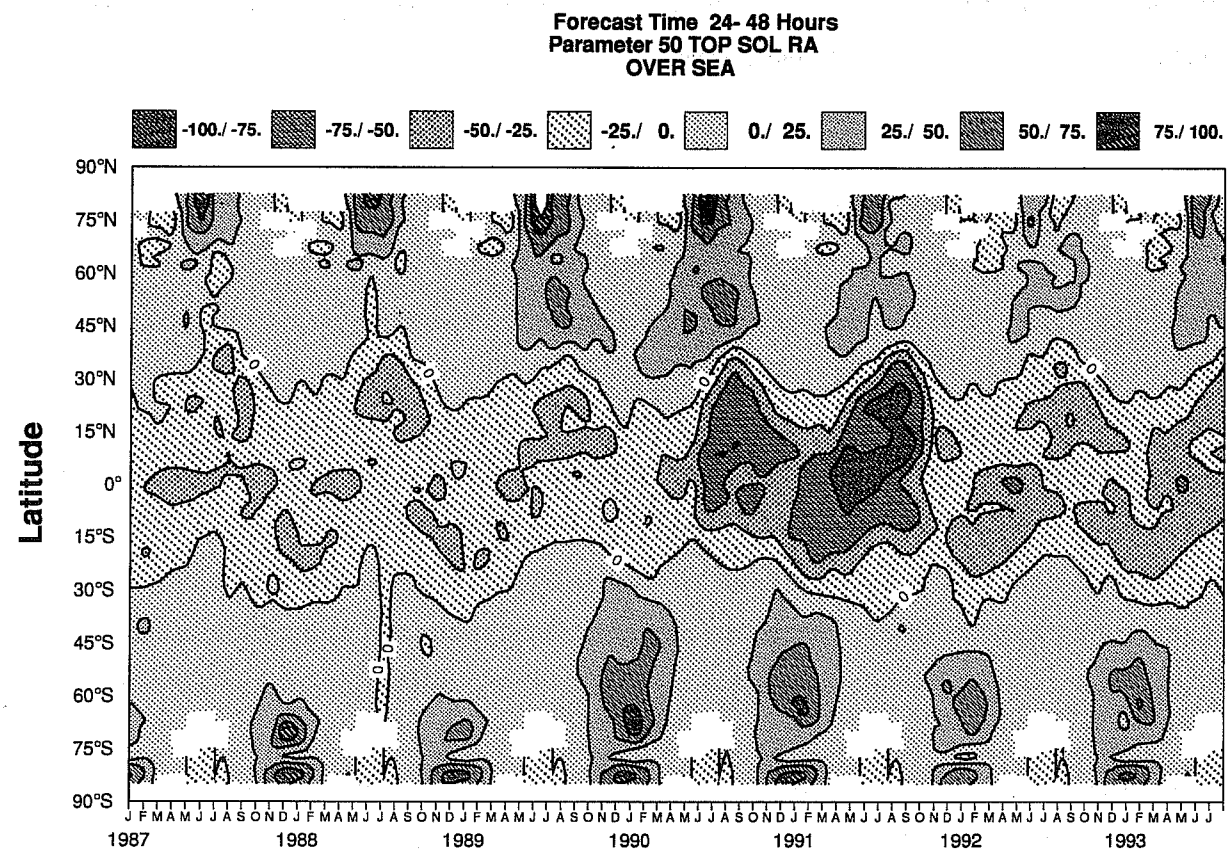

Fig. 5: Monthly and zonal mean differences between ERBE and model net solar radiation at the top of the atmosphere. Zonal averages are calculated for sea points only. Units: Watts/m^2.

tropics changed to a positive bias. Important modifications included the diagnosis of cloud layers, the cloud overlap assumption and the liquid water content of different clouds. In mid-latitudes the high resolution model produced an overestimation of the net thermal radiation. From other diagnostic studies and especially from budget calculations it became clear that the radiative cooling at the top of the troposphere was too large. The effect of reduced liquid water in the anvil clouds in February 1993 shows as an increased bias in the tropical OLR after that time.

For the net solar radiation at the top of the atmosphere the deviations of model values from observations are fairly uniform (Fig. 5). Negative differences suggest that tropical clouds are generally too reflective. Recent investigations of this problem (personal communications with M. Tiedtke) seem to suggest that the negative bias could be reduced by something like 40-60 Watts/m^2 if the appropriate weights of optical properties from different cloud types would be taken into account to calculate the average optical properties of an cloud ensemble.

The model change in June 1990 and April 1991 had a similar affect on the short wave radiation as it had on the long wave radiation. The modification of cloud cover and cloud liquid water increased the amount of short wave radiation reflected back to space which resulted in an increased negative bias compared to ERBE observations from mid-1990 to mid-1991. In the extra-tropics large positive differences are found during the summer season. Insufficient cloud cover suggests that too much solar radiation is absorbed in the extra-tropical oceans.

2.2 Geographical distribution of OLR

The spatial variation of OLR is to a large extent determined by the distribution of cloud cover. Cirrus clouds, which tend to be less opaque than clouds at lower levels, influence the short wave radiation budget only to a limited extent. However, they strongly modulate the long wave radiation budget as they occur at levels where the temperature is relatively low compared to surface temperatures. The high correlation between cloud top temperature and emitted long wave radiation is very useful in identifying areas of deep convection. Maps of monthly mean OLR provide a good estimate of the convective activity in the tropics. The comparison of monthly mean OLR measured from satellite is therefore widely used to validate certain aspects of the hydrological cycle in large scale models.

A useful way of displaying the effects of clouds directly is to show the difference between clear sky fluxes and cloudy fluxes. This so called cloud forcing for long wave radiation (Fig. 6) exhibits the strong effect of deep convective clouds in the tropical convergence zone in reducing the outgoing long-

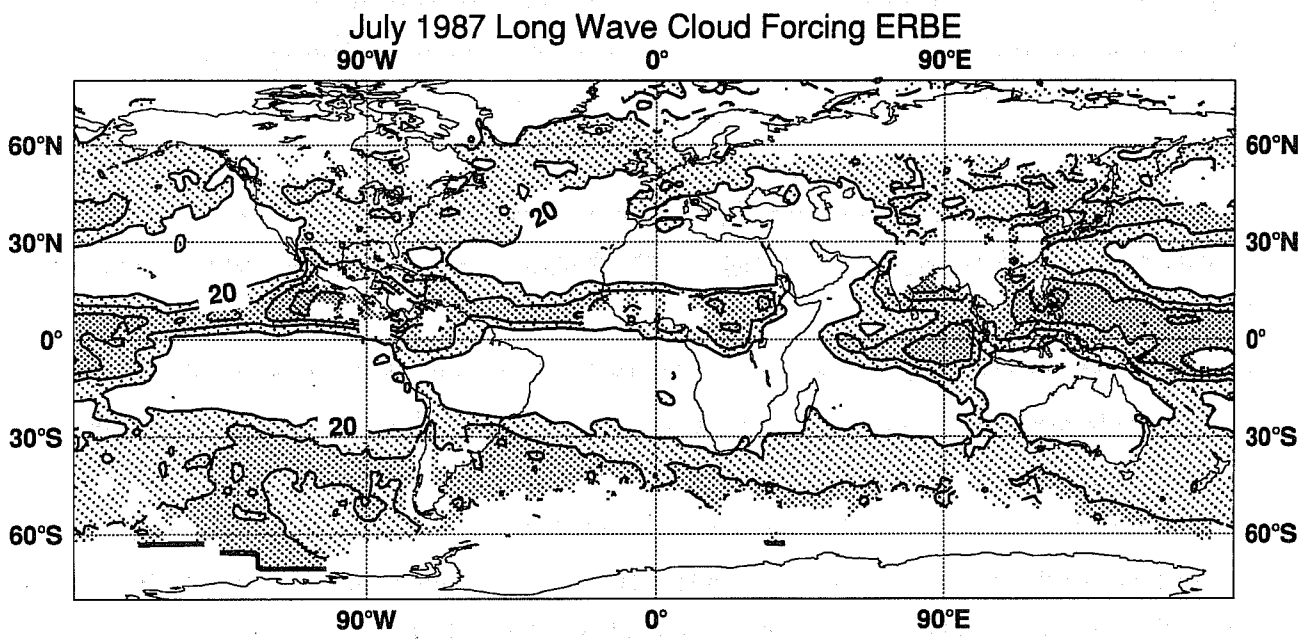

Fig. 6: Monthly mean long-wave cloud forcing from ERBE measurements for July 1987. Contour interval: 20 Watts/m^2.

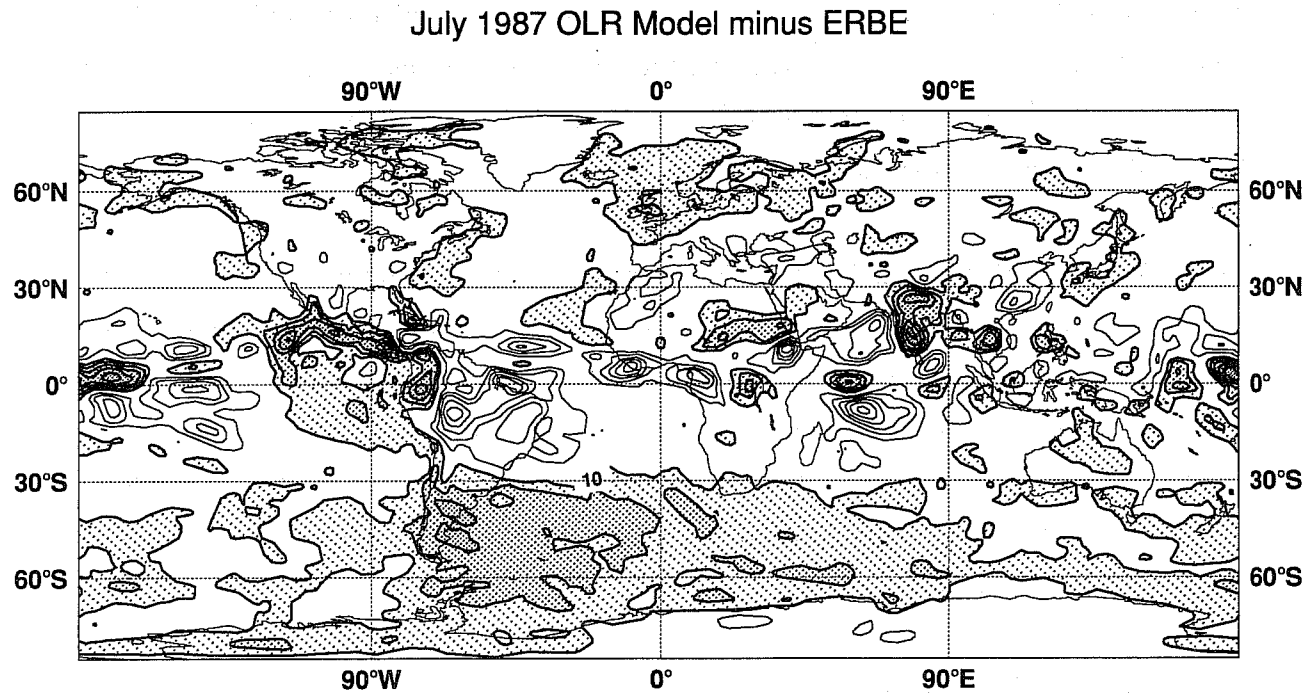

Fig. 7: Difference between monthly mean ERBE and model OLR from short range forecasts for July 1987. Contour interval 10 Watts/m^2, positive values shaded.

wave radiation. Other geographical areas of relatively large cloud forcing are the extra-tropical storm tracks over the ocean and land regions away from the influence of the subtropical highs. Whereas in the tropics clouds reduce the OLR by up to 120 Watts/m^2, the extra-tropical cloud forcing is only in the order of 20 to 40 Watts/m^2.

Systematic model errors in the cloud forcing are almost identical to errors in total long wave fluxes, as clear sky model fluxes agree fairly closely to ERBE observations. Thus the model bias for OLR (Fig. 7) is almost exclusively a bias in the cloud forcing. Systematic differences between model OLR and ERBE data appear mainly in the tropics. An underestimation of OLR can be found over most parts of the tropical convergence zone, particularly over South America, the Atlantic, western parts of Central Africa and the Ethiopian mountains. The dipole pattern of differences in the Indian Ocean suggests that the maximum of convective activity in the model is shifted to the south compared to observations. At the west coast of India the model seems to have generated a spurious maximum of OLR. The fact that a marked coastal model rainfall maximum in the monsoon season is well supported by observation suggests that the model convection is too deep. Further in the western Pacific the model OLR agrees fairly well with observation whereas in the central Pacific the model overestimates the split of the ITCZ.

Large areas of positive deviations from ERBE OLR measurements are found in the Southern Hemisphere storm track and parts of the Northern Hemisphere storm track as well. The suggestion of insufficient cloud forcing in the extra-tropical cyclones is supported by calculations of the model's heat budget, which indicates insufficient diabatic heating from large scale condensation in the short range forecast. Over the Northern Hemisphere land areas the model bias is fairly small. Generally positive values indicate again a possible small underestimation of cloud cover.

The negative bias of OLR diagnosed for the data assimilation experiment for July 1987 and experience with the operational model in 1991 and 1992 led to a revision of some optical properties of clouds. One important part of this change was a reduction of cloud liquid water in the anvil clouds over deep convective towers which made the cirrus clouds more transparent. A simultaneous validation of this model version with ERBE data from 1987 was done by running a single integration for a month from the beginning of July 1987 as initial conditions and the observed sea surface temperature as part of the lower boundary conditions.

Fig. 8 shows the difference between the OLR from the extended integration and ERBE observations. In the extra-tropics the validation of such a long integration is difficult as the model can drift into a flow regime that is completely different from the observed one. However, almost the entire the

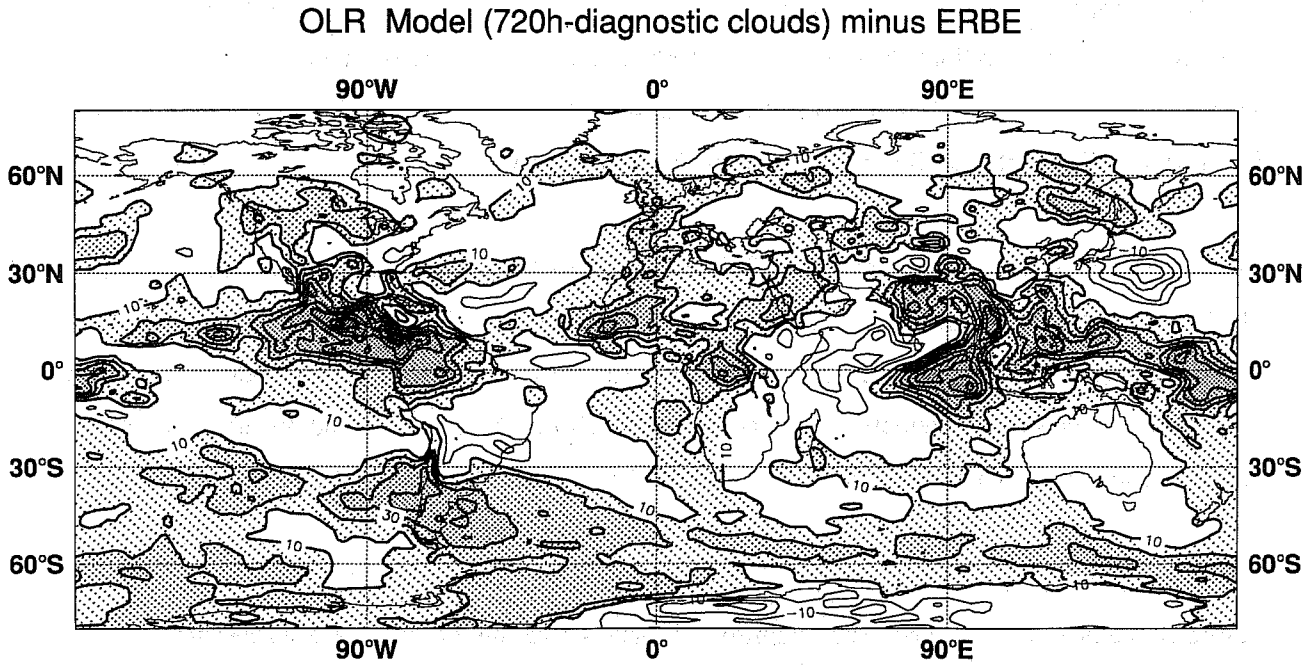

Fig. 8: Difference between monthly mean ERBE and model OLR from a 30 day integration run with a diagnostic cloud scheme for July 1987. Contour interval 10 Watts/m^2, positive values shaded.

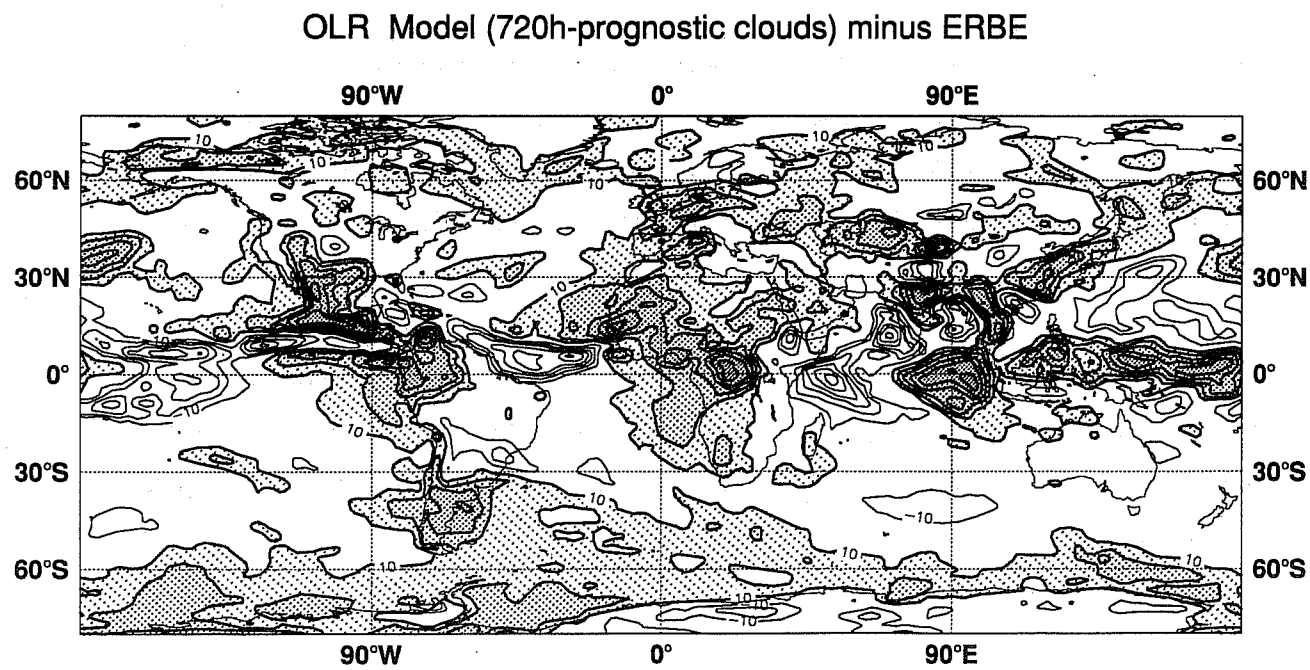

Fig. 9: The same as Fig. 8, except that the model was run with a prognostic cloud scheme.

Southern Hemisphere storm track area shows a similar lack of long wave cloud forcing as seen from the short range forecasts for July 1987. In the tropics, where the flow has a large stationary component, such integrations supply useful information about systematic model errors. The overall impression is that the model OLR represents now an overestimate in most regions of the tropics. Only in the Indian Ocean the satellite measurements show higher values.

The experience of the last few years at ECMWF shows that the performance of the model regarding OLR is very much dependent on the specification of parameters in the diagnostic cloud scheme. Various changes of physical parametrization schemes for surface heat fluxes, convection and radiation were made to improve systematic temperature errors. Those changes also had an effect on cloud-radiation interaction which required an adjustment of the diagnostic cloud scheme.

The cloud fields in the ECMWF scheme (*Slingo*, 1987) are linked to large scale properties like relative humidity, vertical velocity and static stability. Schemes like this are widely used because of their simplicity and relative success in simulating quite well most types of clouds. However, the decoupling of diagnostic cloud schemes from the hydrological cycle limits the improvement that can be gained from future modifications. A better representation of cloud related processes can be achieved in a scheme in which the cloud properties are treated as prognostic parameters. The prognostic cloud scheme that is currently being developed at ECMWF (*Tiedtke*, 1993) defines the time evolution of clouds from the large-scale budget equations of cloud water content and cloud air.

The extended integration for July 1987 with the experimental version of the prognostic cloud scheme shows a noticeable impact on the long wave radiation budget (Fig. 9). Over most areas the OLR has been reduced compared to the diagnostic cloud scheme. Over the tropical oceans, the prognostic cloud scheme underestimates the OLR whereas over land areas the long-wave radiation escaping into space is still too high.

A noticeable difference can also be seen in the extra-tropics. Whereas the diagnostic cloud scheme had insufficient cloud forcing over large areas, particularly over the Southern Hemisphere storm track, the prognostic cloud scheme seems to produce more realistic values of cloud forcing for extra-tropical cloud systems.

2.3 Geographical distribution of short wave radiation

The solar radiation budget is largely affected by clouds of high optical thickness at all levels.

Therefore large values of short wave cloud forcing are found in the tropics from deep convective clouds and from clouds in the extra-tropical storm tracks (Fig. 10). These two areas are separated by minimum cloud forcing in the subtropical highs. Short wave cloud forcing can also be seen from the coastal stratocumulus decks at the eastern sides of the continents.

As for the long wave radiation it can be assumed that errors in the clear sky short wave radiation fluxes are small compared to cloudy fluxes, which means that errors in the cloud forcing and in the net short wave radiation fluxes are almost identical. Therefore the differences between model values and ERBE observations are only shown for the net short wave radiation (Fig. 11). In the tropics the model bias against ERBE observations in the short wave band has a horizontal structure very much like the model bias in the long wave band. Obviously deep convective clouds with their cold anvils modulate different parts of the radiation budget in a similar way by reducing the net downward solar fluxes and the net upward long wave fluxes at the top of the atmosphere. The bias in the short wave radiation suggests that the albedo of tropical clouds is too high. At this point it is difficult to decide whether the problem arises from the definition of optical properties or from the partial cloud cover.

The influence of low level clouds can be seen in some extra-tropical areas. Spurious low levels clouds in the model formulation of July 1991 caused a large reduction of short wave radiation in the Mediterranean. A similar error occurs at the coast of California. A model change in August 1992 redefined the low level inversion clouds. In the revised parametrization inversion clouds were not allowed to exist below the fourth lowest level (level 28, 940 hPa), whereas the search for inversions on which clouds could form was extended upwards to model level 16 (417 hPa). The changed parametrization of the inversion clouds removed some spurious low-level single layer maxima of persistent cloud cover and improved the local thermal balance and the radiation budget.

Other coastal areas like the west coast of Central Africa and South America suggests insufficient cloud forcing in the short wave spectrum. In agreement with results obtained from the ASTEX experiment (Klinker, 1993) it seems that the model underestimates the cloud cover of maritime stratocumulus. Similar to the long wave radiation budget a lack of cloud forcing can also be seen in parts of the oceanic storm track region. Further areas of an underestimation of cloud forcing are the Northern Hemisphere land masses. Excessive absorption of solar radiation causes a positive low level temperature bias in the summer.

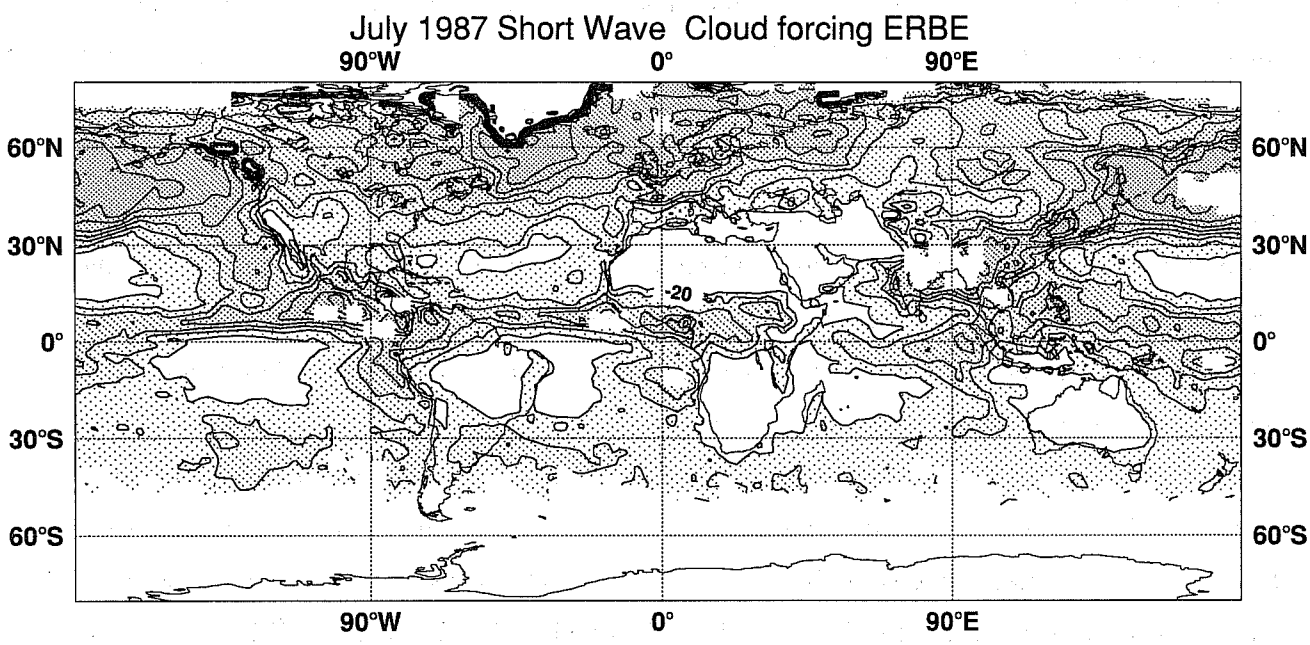

Fig. 10: Monthly mean short-wave cloud forcing from ERBE measurements for July 1987. Contour interval: 20 Watts/m^2.

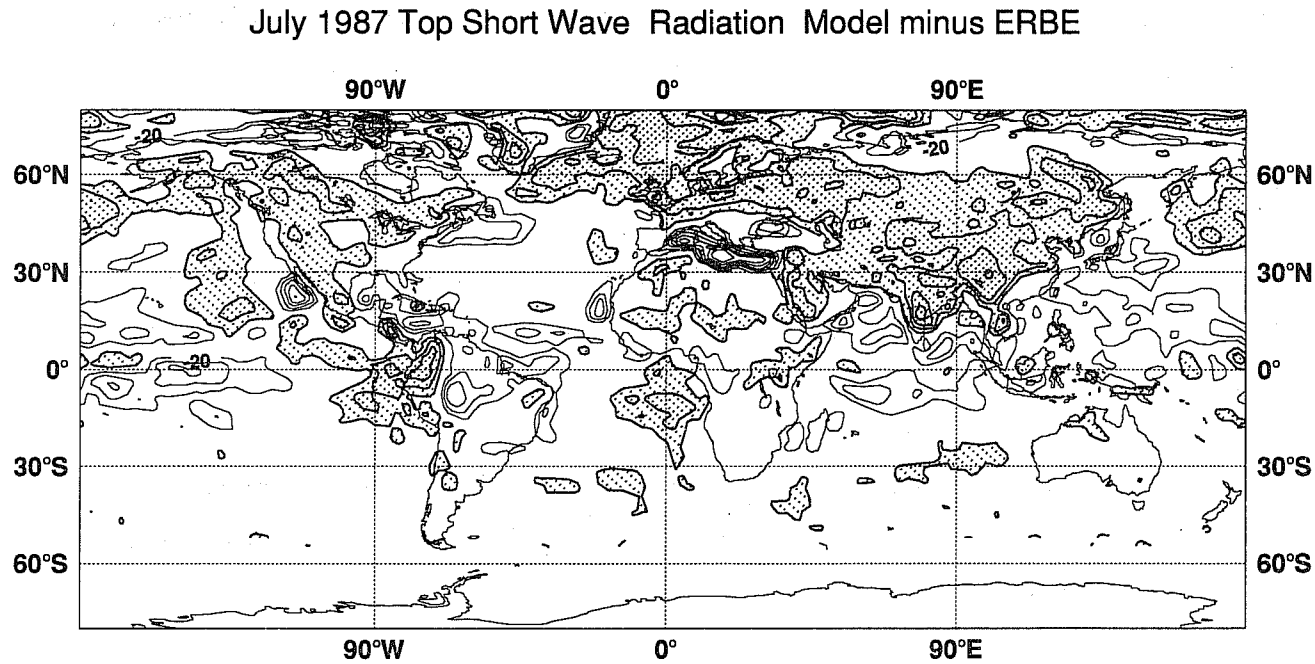

Fig. 11: Difference between monthly mean ERBE and model short-wave radiation at the top of the atmosphere from short range forecasts for July 1987. Contour interval 10 Watts/m^2, positive values shaded.

3. CLOUD VALIDATION

There is a variety of cloud observations available which is suitable for the validation of cloud cover produced by large scale models. At ECMWF the cloud information from the synoptic reports is used to monitor the performance of the current operational model. Though these reports are mostly based on subjective estimates, experience at ECMWF has shown that the data is accurate enough to reveal model biases. In particular, systematic model errors in cloud cover correlate well with systematic low level temperature errors.

Field experiments are often designed to investigate certain types of clouds. Despite the limited time and space coverage of measurements in campaigns like this, they can provide useful guidance for the parametrization of clouds. ECMWF has been involved in supporting the Atlantic Stratocumulus Transition Experiment (ASTEX) which was carried out in the East Atlantic during June 1992. The first results reveal problems in the parametrization of low level inversion clouds (Klinker, 1993). It seems that the assumption in the cloud parametrization, that there is a good relation between the strength of the inversion, the relative humidity and cloud cover, is not supported by data. The result is a poor correlation between observed and forecast low level maritime cloud cover and a general underestimation of cloud amounts.

Global validation of clouds is only possible by using satellite data. The International Satellite Cloud Climatology Project (ISCCP) was established to produce high quality global data-sets of infrared and visible radiances (Rossow and Garder, 1993) from which cloud properties have been derived. Similar to ERBE products, there is a considerable lag between the observation time and the time the cloud products are available for model validation. The cloud schemes, either the presently operational diagnostic cloud scheme (Slingo, 1987, DCC) or the new prognostic cloud scheme (Tiedtke, 1993, PCC) can only be validated by running forecast experiments from past initial dates or by performing a complete data-assimilation experiment.

3.1 Cloud cover

In the International Satellite Cloud Climatology Project databases (Rossow et al., 1987, 1988), the longwave window and shortwave radiances represent the original information. All other cloud parameters (cloud top pressure/temperature, optical thickness, ...) are data derived from the radiances with the help of the ISCCP radiation scheme that differs from the ECMWF model radiation scheme, and that may differ from the actual truth. However, given the amplitude of some of the errors in the model cloud parameters, the ISCCP-C1 data provides very useful information for model validation (Tiedtke, 1993), provided the following limitations are acknowledged:

(a) In essence, the only consistent way to validate model clouds would be to simulate satellite radiances from the model outputs and to compare the observed and simulated radiances. This is a powerful way for studying the model cloud-radiation interactions (Morcrette, 1991b). However, if the emphasis is put on cloud fraction, cloud top temperature/pressure, consistency would require to process the model simulated radiances with the same algorithm used for processing the observed radiances. A first step in that direction is to recognize that the ISCCP-C1 clouds have a radiative definition, i.e., clouds are detected from the modifications that they bring to the clear-sky radiances. Thus, a more meaningful comparison with observations should be that of the model cloudiness as it is seen by the model radiation scheme.

The importance of taking the radiative properties of clouds into account becomes clear by comparing the ISCCP C1 high cloudiness (Fig. 12) derived from only IR measurements, with both the PCC model high cloudiness (Fig. 13) and the model high effective cloudiness (Fig. 14) where the cloud fraction in each model layer is weighted by its longwave emissivity. The ISCCP high levelclouds are defined to occur between the top of the atmosphere and 440 hPa, whereas the model high cloudiness corresponds to clouds between the top of the atmosphere and a sigma level of 0.45. The much smaller cover by high effective cloudiness relative to that by high cloudiness shows that a large fraction of the model high cloudiness corresponds to low liquid/ice water loading with resulting small longwave emissivities and small radiative impact. This feature obviously affects the total effective cloudiness as well.

(b) Due to the overlapping of cloud layers, the ISCCP-C1 estimates of clouds other than the highest ones must be regarded as lower limits; thus, model clouds have to be processed to simulate the overlapping by higher cloud layers for a meaningful comparison of model-generated and satellite-derived low and medium-level cloudiness. For low-level clouds (surface to 800 hPa for ISCCP, between surface and sigma = 0.8 for the model) and medium-level clouds (between 800 and 440 hPa for ISCCP, and between sigma = 0.8 and 0.45 for the model), such comparisons are presented in Figs. 15 to 18. The low-level cloud comparison clearly shows another difficulty in this type of comparisons as the height/pressure/temperature assignment of the ISCCP clouds may systematically differ from that of the model clouds because of deficiencies in the ISCCP analysis (e.g., NMC temperature profiles have too small subtropical temperature inversions, which has the effect of locating low clouds too high; optically thin high clouds over optically thick lower clouds are located too low). The stratocumulus decks off-coast the western facades of the continents in the subtropics (Fig. 16 for the model low clouds) do not appear in the ISCPP low clouds (Fig. 15) but have been attributed cloud top pressure that make them part of the medium-level clouds (Fig. 17).

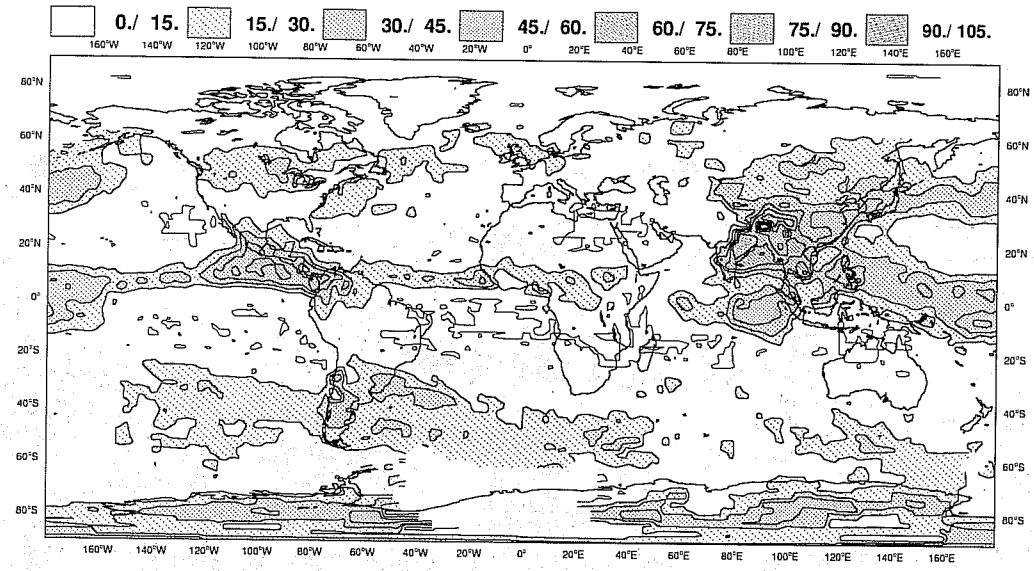

Fig. 12: Cloud cover derived from ISCCP long wave window radiances for high-level clouds (cloud-top pressure lower than 440 hPa). The average is performed over 31 files corresponding to the 12 GMT imagery for July 1987.

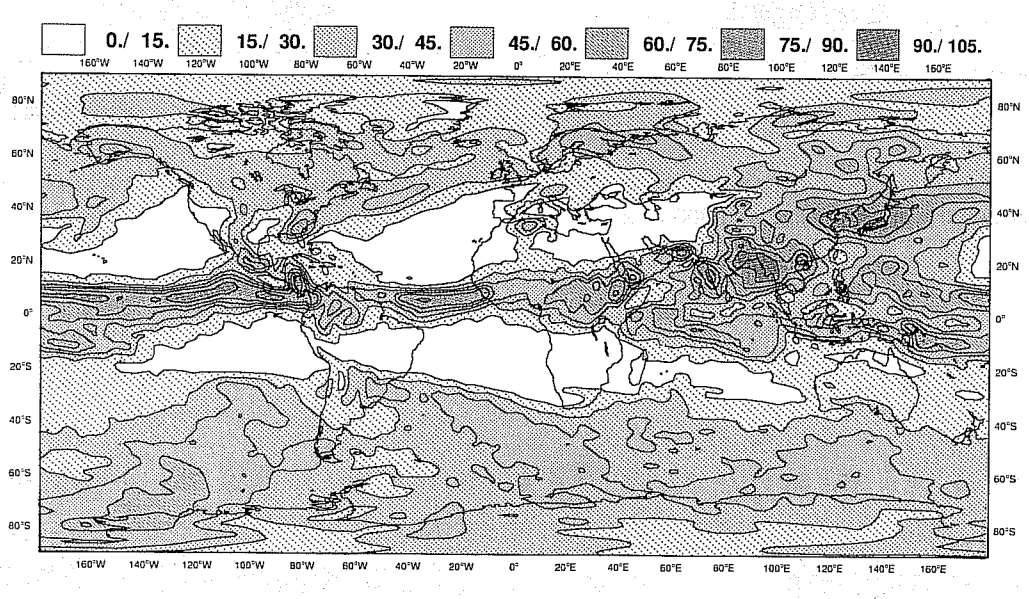

Fig. 13: Cloud cover obtained from the ECMWF model simulation of July 1987 for high clouds (between $\sigma = 0.45$ and the top of the atmosphere). Only 12 GMT time steps are considered. The T63 L31 (cy 46) model includes the prognostic cloud scheme from Tiedtke (1993). Cloud overlap assumption is the operationally used maximum-random overlap assumption.

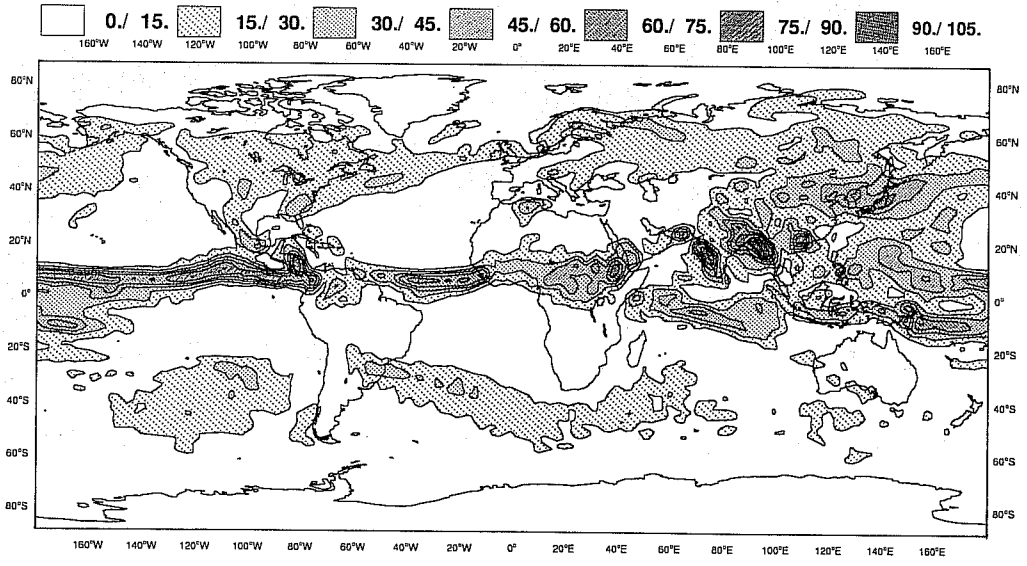

Fig. 14: As in Fig. 13, but for the model high-level effective cloudiness.

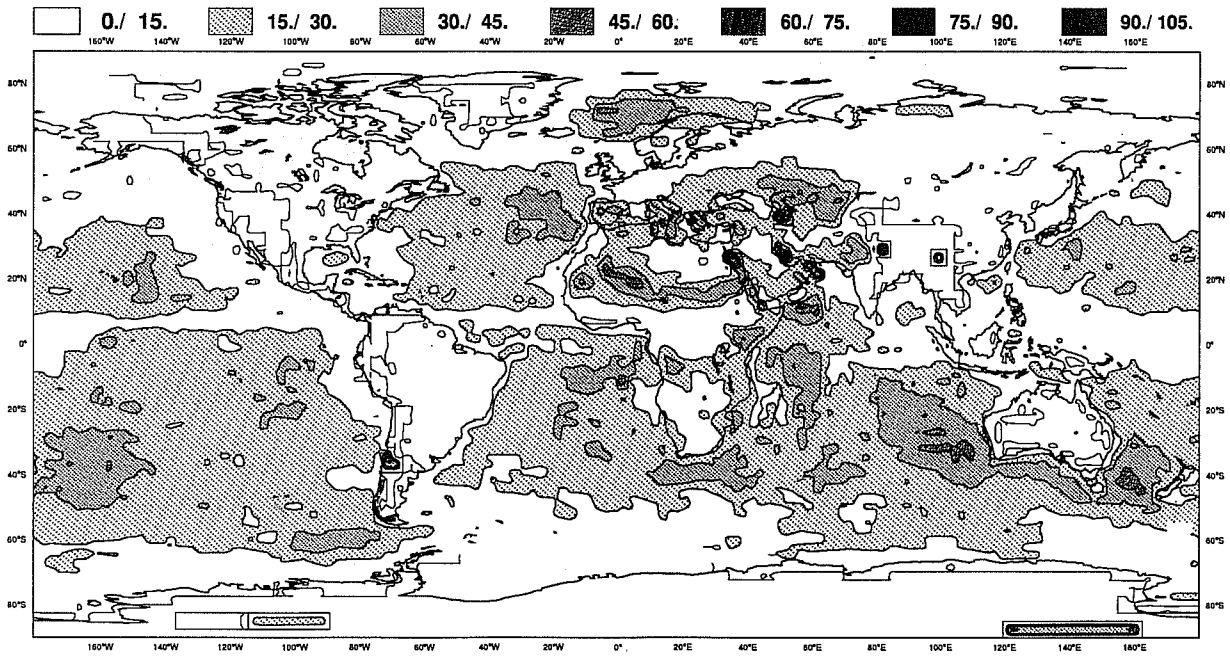

Fig. 15: The low-level cloudiness derived from ISCCP long wave window radiances only. Cloud top pressures are located between the surface value and 800 hPa.

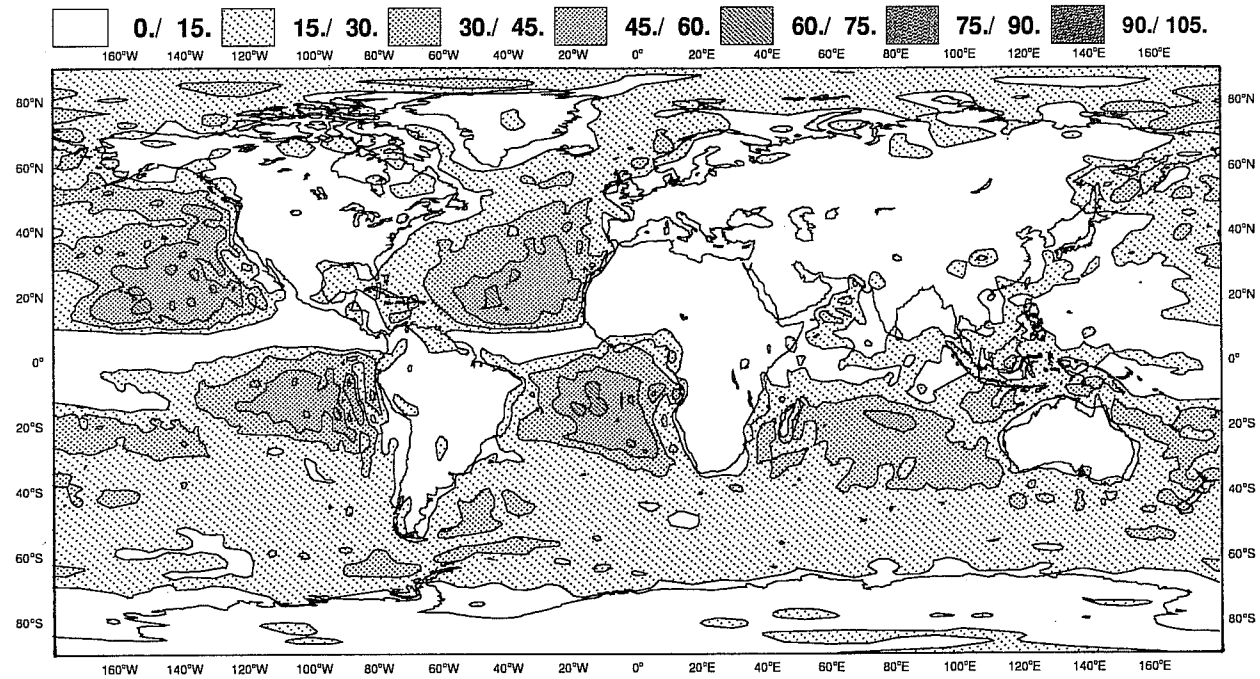

Fig. 16: The model low-level cloudiness, between the surface and $\sigma = 0.8$, not obscured by higher-level clouds.

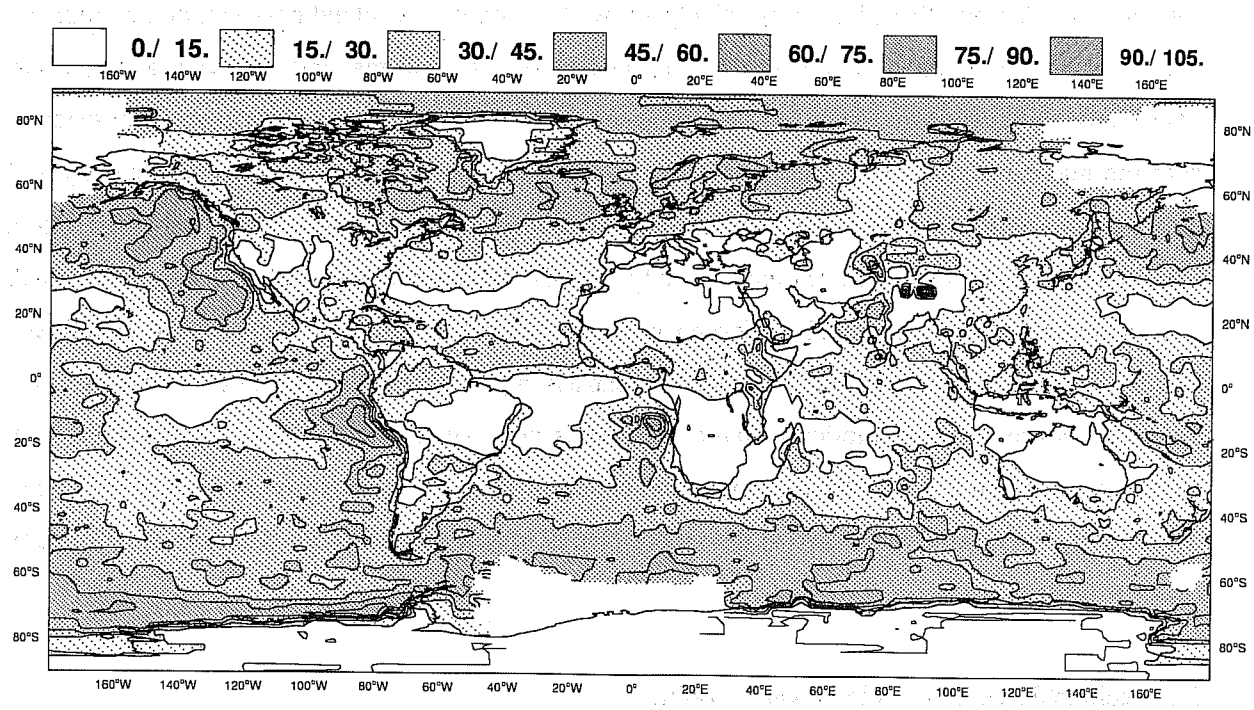

Fig. 17: The medium-level cloudiness derived from ISCCP long wave window radiances only. Cloud top pressures are located between 800 and 440 hPa.

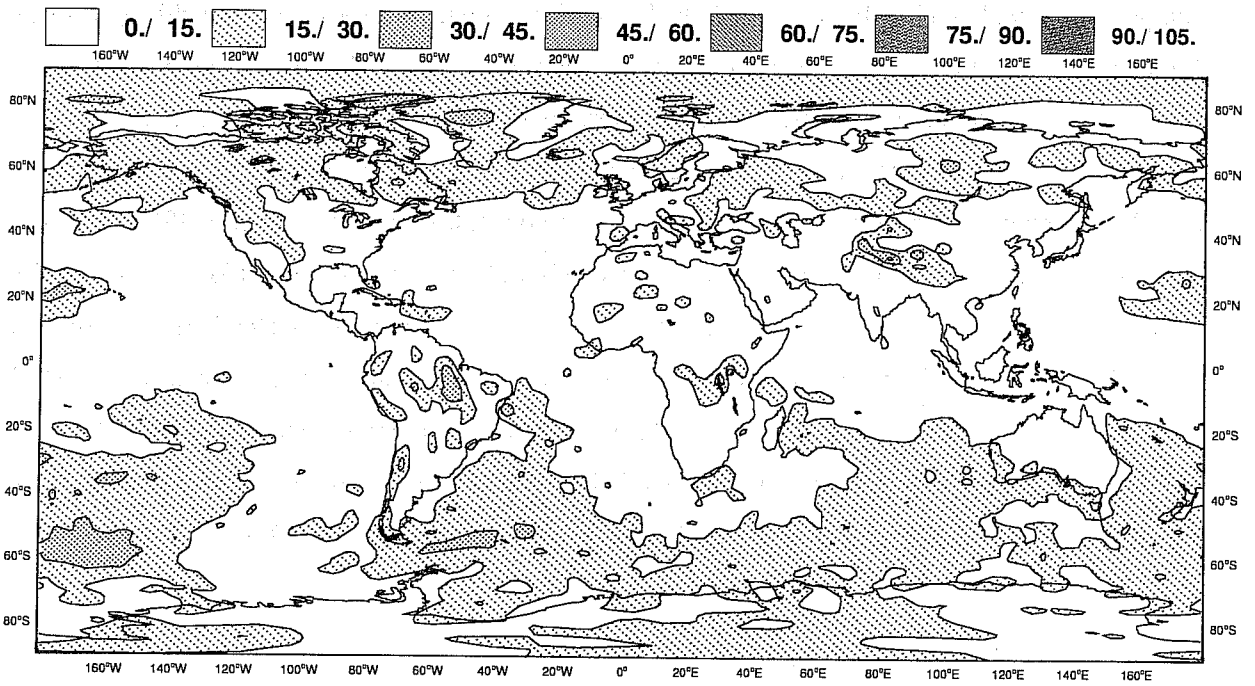

Fig. 18: The model medium-level cloudiness, between $\sigma = 0.8$ and $\sigma = 0.45$, not obscured by higher-level clouds.

A related topic concerns the overlap assumption used to compare the model cloudiness to the satellite-derived one. Figures 20 and 21 respectively show the model total cloudiness computed from the individual layer fractional cloudiness with the random overlap and maximum overlap assumptions. These have to be compared with Fig. 19 where the model total cloudiness is computed consistently with the maximum-random overlap assumption used in the operational radiation scheme. By and large, the maximum-random and maximum overlap assumptions give similar results, showing that a large fraction of the model clouds are vertically organized. The random overlap assumption, which considers clouds to be statistically independent in the vertical, gives much higher total cloudiness. Overall, in the tropics, the maximum-random overlap assumption gives results only slightly higher than the maximum overlap assumption as the cloudiness is dominated by convective cloud towers, with only little occurrence of stratiform clouds disconnected from the convective processes. At higher latitudes, there is more variability as the model clouds may appear as more than one set of cloudy adjacent layers.

3.2 Precipitable water and cloud water loading

Information on the total precipitable water and cloud liquid water loading can be derived from microwave observations (SSM/I). They are now used to validate the vertically integrated water vapour in the ECMWF model (Morcrette et al., 1991; Tiedtke, 1993). The model validation presented here is based on extended integrations using the new prognostic cloud formulation. Figures 22 and 23 compare the model precipitable water with the SSM/I derived one, and shows a reasonable agreement. Validation of the cloud water content produced in the model is more difficult as the present SSM/I channels and algorithms do not provide reliable information on cloud ice water content, and as the observed cloud liquid water might be contaminated by rain water in areas of heavy precipitation (ITCZ, mid-latitude storm tracks). The cloud shortwave optical thicknesses reported in ISCCP C1 data can also be translated into a vertically integrated cloud liquid water path (Drake, 1993), as the ISCCP radiation scheme used in the retrieval of the cloud optical thickness assumes clouds that are formed only by 10 μm water droplets. Figures 24 to 26 presents the total cloud water derived from SSM/I (Fig. 24), from ISCCP-C1 (Fig. 25), and from the ECMWF PCC model integration (Fig. 26). The PCC model is in rough agreement with the SSM/I data, but the value of such an agreement is largely questioned when considering the much smaller values derived from the ISCCP C1 observations.

4. Conclusion

Satellite observations as any other type of observations can provide constraints for the verification of

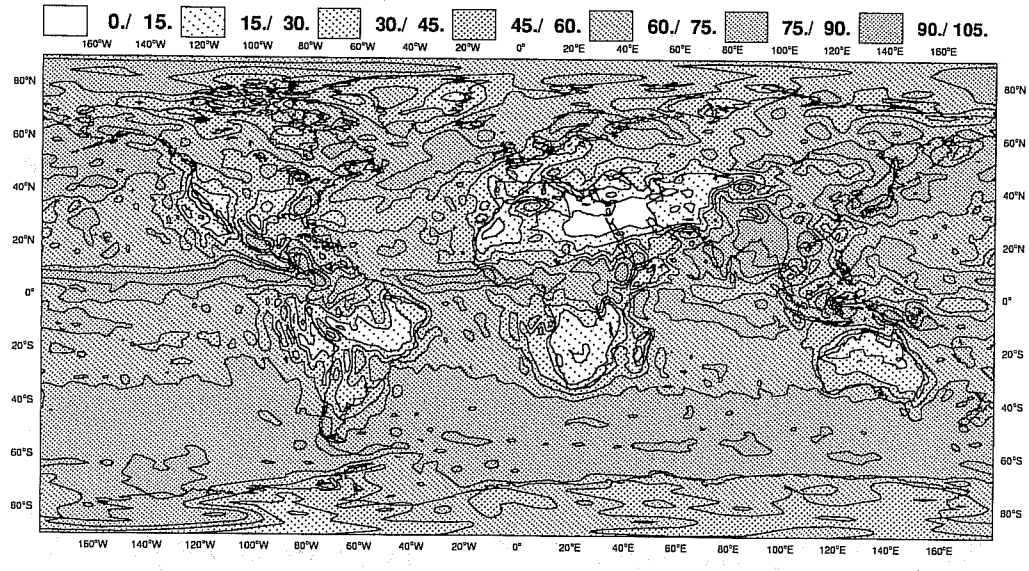

Fig. 19: The total cloudiness obtained from the ECMWF model simulation of July 1987. Only 12 GMT time steps are considered. The T63 L31 (cy 46) model includes the prognostic cloud scheme from Tiedtke (1993). Cloud overlap assumption is the operationally used maximum-random overlap assumption.

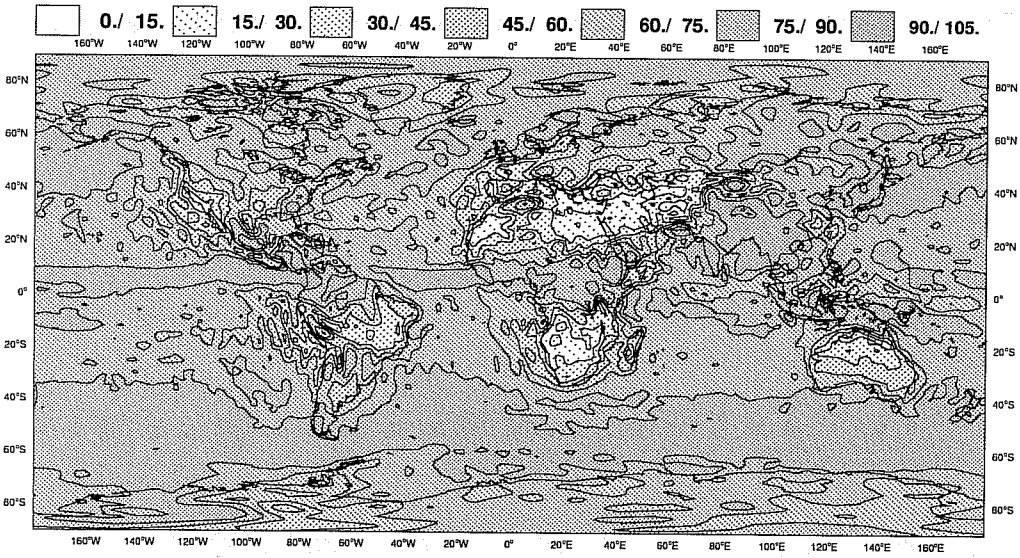

Fig. 20: As in Fig.19, but computation of the total cloudiness is performed assuming a random overlapping of cloud layers.

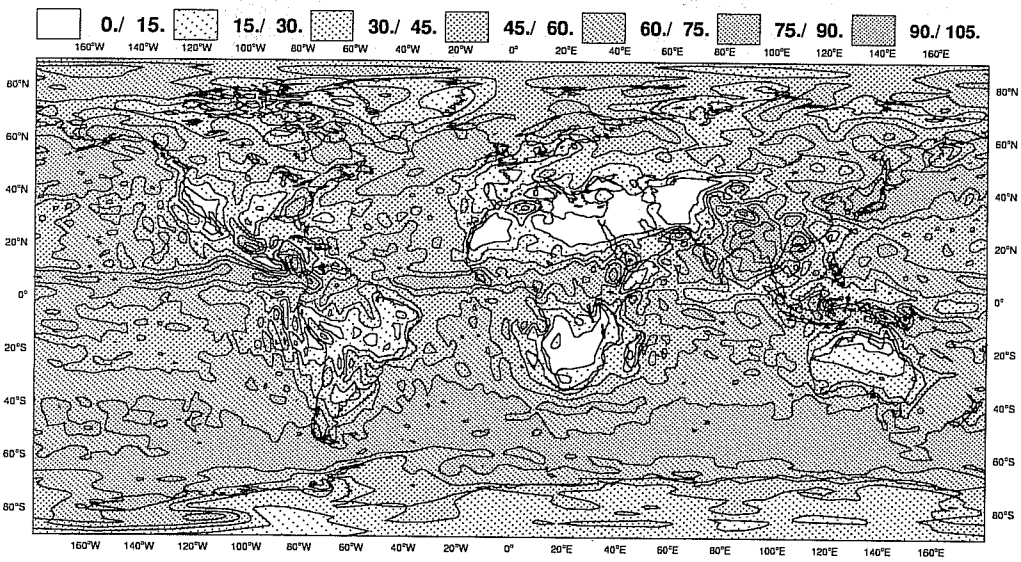

Fig. 21: As in Fig.19, but computation of the model total cloudiness is performed assuming a maximum overlapping of cloud layers.

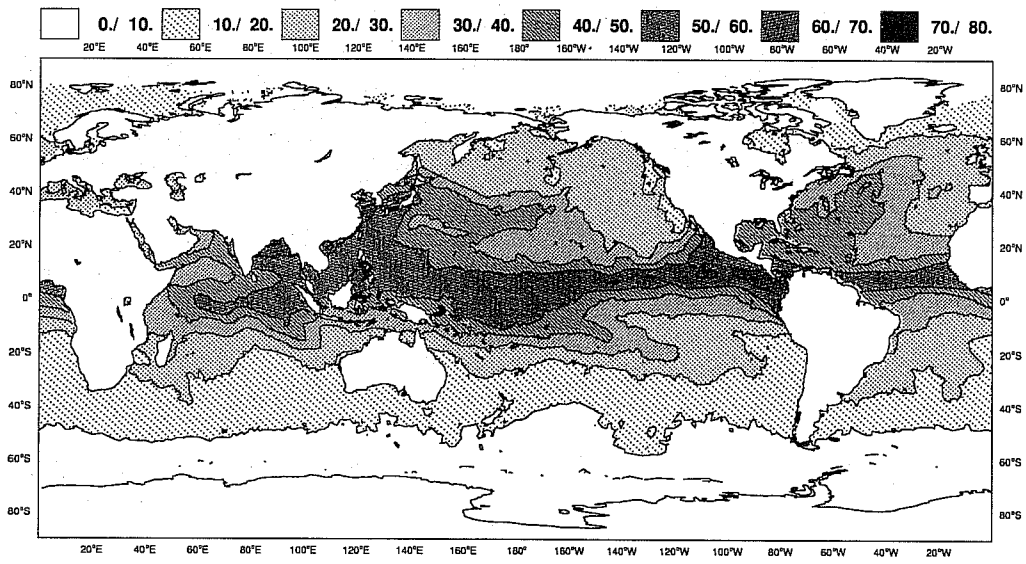

Fig. 22: The precipitable water derived from SSM/I measurements over the 9 to 31 July 1987 period (in kg.m^{-2}).

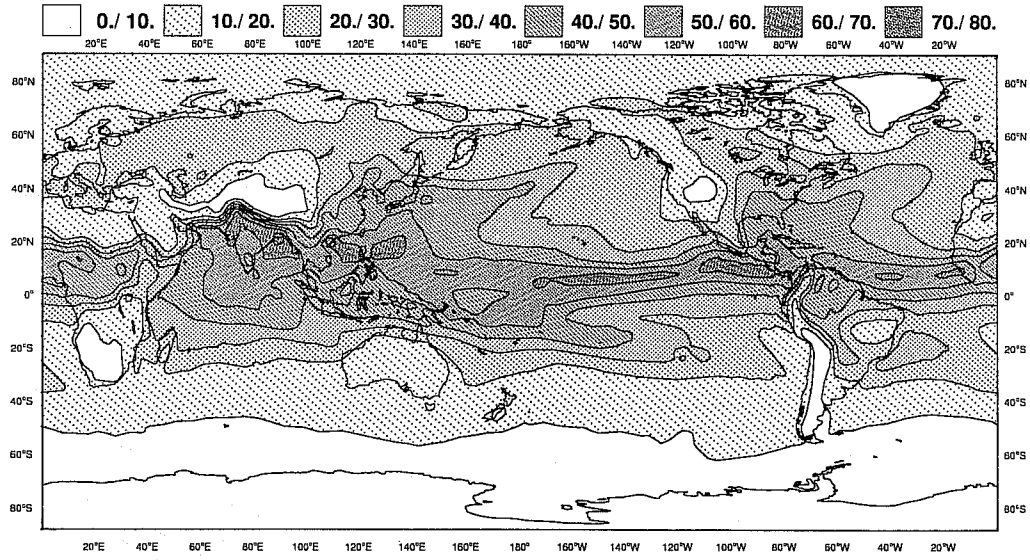

Fig. 23: The precipitable water from a July 1987 model simulation averaged over the 9 to 31 July period (in kg.m^{-2}).

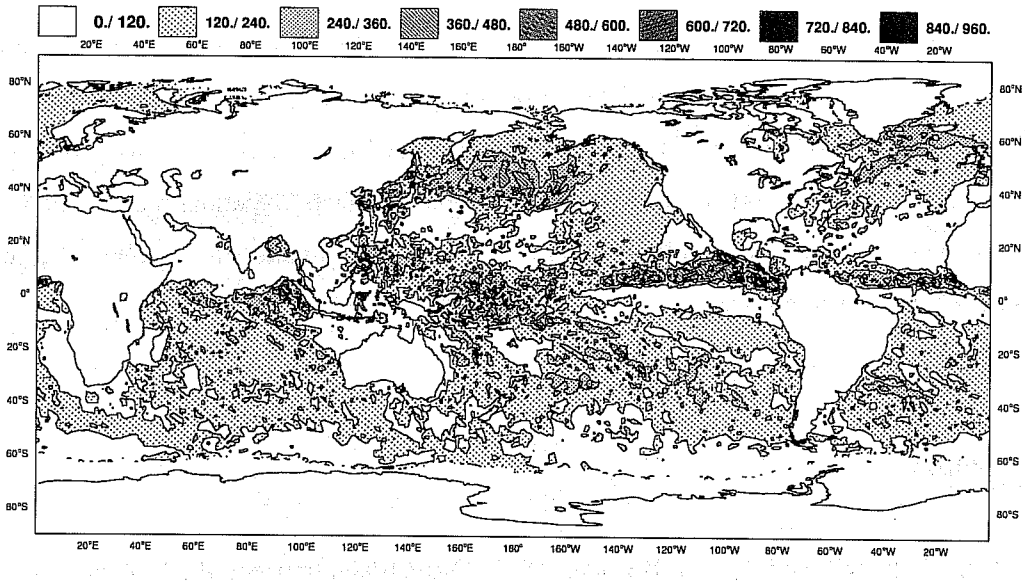

Fig. 24: The total cloud water derived from SSM/I measurements over the 9 to 31 July 1987 period (in $g.m^{-2}$).

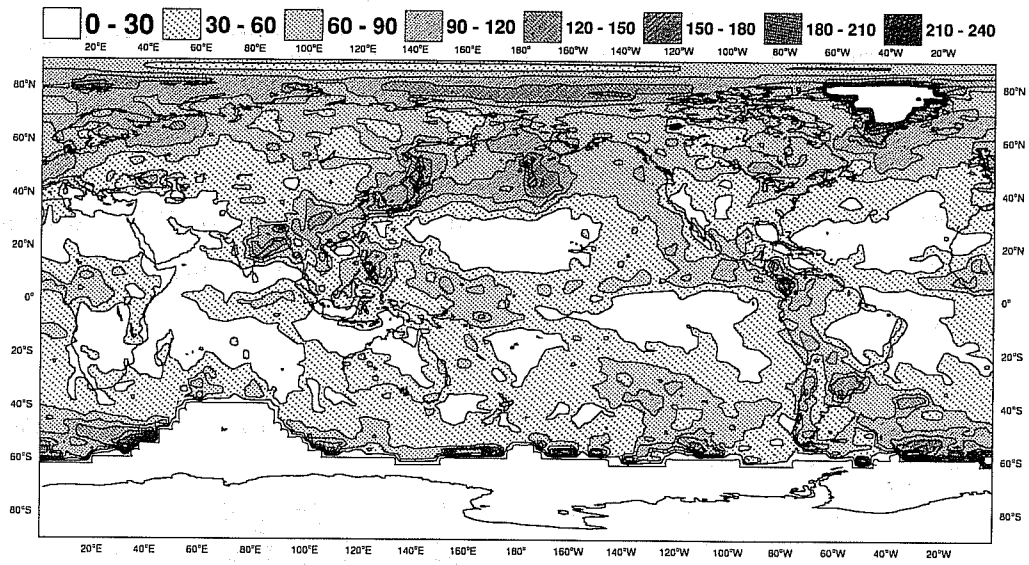

Fig. 25: The total cloud water derived from the ISCCP C1 shortwave cloud optical thickness (in $g.m^{-2)}$.

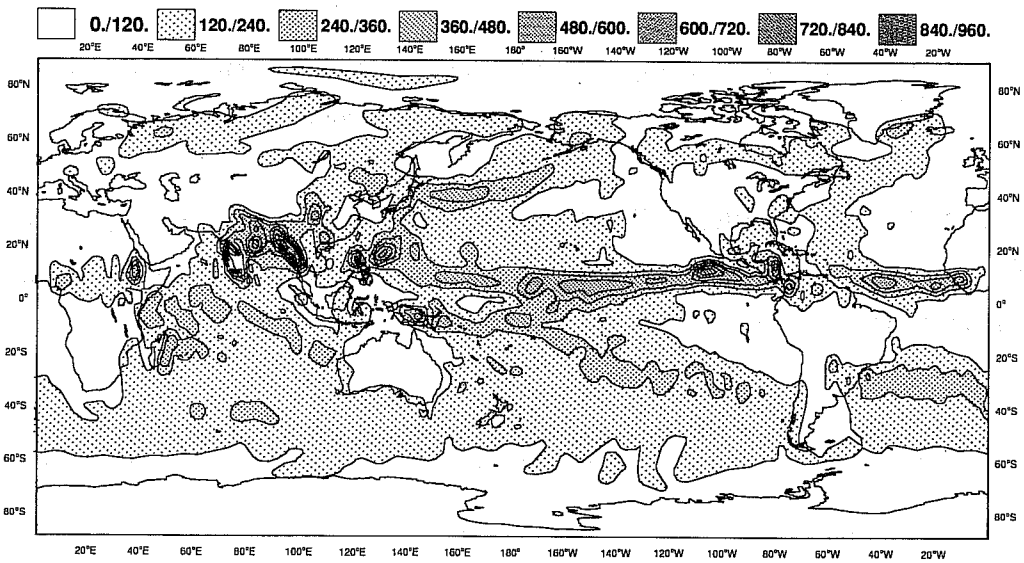

Fig. 26: The total cloud water from a July 1987 model simulation averaged over the 9 to 31 July period (in $g.m^{-2}$).

some aspects of the output of a large scale atmospheric model. Due to their intrinsic characteristics, their global coverage and their good temporal sampling, they provide a first order tool for the verification of the cloud-radiation interactions parameterized in a GCM. The synergy brought by their use in conjunction with other types of observations (surface radiation measurements, synoptic meteorological observations, radiosoundings, ...) allows the validation/verification of a much wider range of physical parametrizations.

5. References

Betts, A.K., J.H. Ball, and A.C.M. Beljaars, 1993: Comparison between the land surface response of the ECMWF model and the FIFE-1987 data. *Quart. J. Roy. Meteor. Soc.*, 119B, 975-1001.

Drake, F., 1993: Global cloud cover and cloud water path from ISCCP C2 data. Intern. J. Climatol., 13, 581-605.

Klinker, 1993: Analysis and diagnostics of the ECMWF model during ASTEX. Proceedings of the workshop on parametrization of the cloud topped boundary layer. 8-11 June 1993. Can be obtained from ECMWF.

Morcrette, J.-J., 1990: Impact of changes to the radiation scheme in the ECMWF model. *Mon.Wea.Rev.*, 118, 857-873.

Morcrette, J.-J., 1991a: Radiation and cloud radiative properties in the ECMWF operational weather forecasting model. *J. Geophys. Res.*, 96D, 9121-9132.

Morcrette, J.-J., 1991b: Evaluation of model-generated cloudiness: Satellite observed and model-generated diurnal variability of brightness temperature. *Mon. Wea. Rev.*, 119, 1205-1224.

Morcrette, J.-J., L. Illari, E. Klinker, H. Le Treut, M. Miller, P. Rasch, and M. Tiedtke, 1991: Clouds and Radiation in the ECMWF model - Recent Developments. ECMWF Technical Memo. No. 181, Reading, U.K., 48 pp.

Rossow, W.B., E. Kinsella, A. Wolf, and L. Garder, 1987: International Satellite Cloud Climatology Project (ISCCP): Description of Reduced Resolution Radiance Data. July 1985 (revised July 1987). WMO/TD-No.58, World Meteorological Organization, Geneva, 143 pp.

Rossow, W.B., L.C. Garder, P.J. Lu, and A.W. Walker, 1988: International Satellite Cloud Climatology Project (ISCCP): Documentation of Cloud Data. WMO/TD-No.266, World Meteorological Organization, Geneva, 78 pp. + 2 appendices.

Rossow, W.B., and L.C. Garder, 1993: Cloud detection using satellite measurements of infrared and visible radiances for ISCCP. J. Climate, 6, 2341-2369.

Rossow, W.B., and L.C. Garder, 1993: Validation of ISCCP cloud detections. J. Climate, 6, 2370-2393.

Slingo, J.M. 1987: The development and verification of a cloud prediction scheme for the ECMWF model. *Quart. J. Roy. Meteor. Soc.*, 113, 899-927.

Tiedtke, M. 1989: A comprehensive mass flux scheme for cumulus parameterization in large scale models. *Mon.Wea.Rev.*, 117, 1779-1800.

Tiedtke, M. 1993: Representation of clouds in large-scale models. *Mon. Wea. Rev.*, 121, 3040-3061.

Webb M.J., Slingo A. and Stephens G.L., 1993: Seasonal variations of the clear-sky greenhouse effect: the role of changes in atmospheric temperaures and humidities. *Climate Dynamics*. In press.